Supplemental Material for

Continuous Time Crystal in Alkali Spin Ensemble Dynamical Phase Transition

Weiyi Wang, Shudong Lin, Yuhao Wang, Zhen Chai, Kai Wei,* and Jiancheng Fang
The School of Instrumentation and Optoelectronic Engineering, Beihang University, Beijing 100191, China
National Institute of Extremely-Weak Magnetic Field Infrastructure, Hangzhou, Zhejiang 310000, China and
Hefei National Laboratory, Hefei, 230088, China

Dmitry Budker
Johannes Gutenberg-Universität Mainz, 55122 Mainz, Germany
Helmholtz Institute Mainz, 55099 Mainz, Germany
GSI Helmholtzzentrum für Schwerionenforschung GmbH, 64291 Darmstadt, Germany and
Department of Physics, University of California,
Berkeley, CA 94720-7300, United States of America

I. DERIVATION OF MASTER EQUATION FOR THERMAL ATOMIC SPIN ENSEMBLE

The density matrix evolution of alkali atoms is given by [1]

$$\frac{d\hat{\rho}}{dt} = -\frac{i}{\hbar}\left[\hat{\mathcal{H}}_0, \hat{\rho}\right] + R_{\rm sd}\left[\hat{\varphi} - \hat{\rho}\right] + R_{\rm se}\left[\hat{\varphi}\left(\mathcal{I} + 4\langle \boldsymbol{S}\rangle \cdot \hat{\boldsymbol{S}}\right) - \hat{\rho}\right] + R_{\rm op}\left[\hat{\varphi}\left(\mathcal{I} + 2\boldsymbol{s}\cdot\hat{\boldsymbol{S}}\right) - \hat{\rho}\right], \tag{S1}$$

where the ground state Hamiltonian $\hat{\mathcal{H}}_0 = A_{\rm hfs}\hat{\boldsymbol{I}}\cdot\hat{\boldsymbol{S}} + g_s\mu_B\boldsymbol{B}\cdot\hat{\boldsymbol{S}} - g_I\mu_I\boldsymbol{B}\cdot\hat{\boldsymbol{I}}$. $\hat{\boldsymbol{S}}$ and $\hat{\boldsymbol{I}}$ are the electron and nuclear spin operators of alkali atom. $\boldsymbol{B}$ is the magnetic field. Pure electron spin operator $\hat{\varphi} = \hat{\rho}/4 + \hat{\boldsymbol{S}}\cdot\rho_e\hat{\boldsymbol{S}}$, where we have neglected light shift term since it can be eliminated by the magnetic field compensation. $R_{\rm se/sd/op}$ is the rate for spin exchange (se) interaction, spin destruction (sd) interactions, and optical pumping (op), respectively. $\langle\mathcal{O}\rangle = {\rm Tr}[\hat{\rho}\hat{\mathcal{O}}]$ is the ensemble average for arbitrary operator $\hat{\mathcal{O}}$. $\mathcal{I}$ is the unitary matrix. $\boldsymbol{s} = i\boldsymbol{E}\times\boldsymbol{E}^*/|\boldsymbol{E}|^2$ is the average photon spin. Here, the first term on the right stands for unitary evolution of $\hat{\mathcal{H}}_0$. The second term is the relaxation process of alkali atoms. The third term is the spin exchange interactions between alkali atoms. The fourth term is the optical pumping process neglecting light shift term. The fourth term is the spin exchange interactions among alkali atoms.

To show that Eq. (S1) can be written in master equation form as Eq. (1) shown in the manuscript, we will show that the last three terms can be simplified to Lindblad terms. We begin from the destruction term $R_{\rm sd}[\hat{\varphi} - \hat{\rho}]$.

$$R_{\rm sd}[\hat{\varphi} - \hat{\rho}] = R_{\rm sd}\left[\hat{\boldsymbol{S}}\cdot\hat{\rho}\hat{\boldsymbol{S}} - \frac{3}{4}\hat{\rho}\right]. \tag{S2}$$

Since $3\hat{\rho}/4 = S(S+1)\hat{\rho} = \hat{\boldsymbol{S}}^2\hat{\rho} = \left(\frac{\hat{S}_+\hat{S}_- + \hat{S}_-\hat{S}_+}{2} + \hat{S}_z^2\right)\hat{\rho} = \left(\frac{\hat{S}_+\hat{S}_- + \hat{S}_-\hat{S}_+}{4} + \frac{\hat{S}_z^2}{2}\right)\hat{\rho} + \hat{\rho}\left(\frac{\hat{S}_+\hat{S}_- + \hat{S}_-\hat{S}_+}{4} + \frac{\hat{S}_z^2}{2}\right) = \frac{1}{2}\left[\frac{\{\hat{S}_-^\dagger\hat{S}_-,\hat{\rho}\}}{2} + \frac{\{\hat{S}_+^\dagger\hat{S}_+,\hat{\rho}\}}{2}\right] + \frac{\{\hat{S}_z^\dagger\hat{S}_z,\hat{\rho}\}}{2}$, we have

$$R_{\rm sd}[\hat{\varphi} - \hat{\rho}] = \frac{R_{\rm sd}}{2}\left[\left(\hat{S}_-\hat{\rho}\hat{S}_-^\dagger - \frac{\{\hat{S}_-^\dagger\hat{S}_-,\hat{\rho}\}}{2}\right) + \left(\hat{S}_+\hat{\rho}\hat{S}_+^\dagger - \frac{\{\hat{S}_+^\dagger\hat{S}_+,\hat{\rho}\}}{2}\right)\right] + R_{\rm sd}\left[\hat{S}_z\rho\hat{S}_z^\dagger - \frac{\{\hat{S}_z^\dagger\hat{S}_z,\hat{\rho}\}}{2}\right]. \tag{S3}$$

In this way, we show that spin destruction interactions can be written in Lindblad form. Similar calculation can be performed to optical pumping. With the Eq. (102) in [1], optical pumping term can be simplified as

$$R_{\rm op}\left[\hat{\varphi}(1 + 2\boldsymbol{s}\cdot\hat{\boldsymbol{S}}) - \hat{\rho}\right] = R_{\rm op}\left[\hat{\boldsymbol{S}}\cdot\hat{\rho}\hat{\boldsymbol{S}} - \frac{3}{4}\hat{\rho}\right] + \frac{R_{\rm op}}{2}\left[\left\{\hat{\rho}, \boldsymbol{s}\cdot\hat{\boldsymbol{S}}\right\} - 2i\boldsymbol{s}\cdot\left(\hat{\boldsymbol{S}}\times\hat{\rho}\hat{\boldsymbol{S}}\right)\right] \tag{S4}$$

* Contact author: weikai@buaa.edu.cn

In consistence to our experiment, we set $\boldsymbol{s} = (0, 0, 1)$. Then we find the equation above can be simplified as

$$\begin{aligned} R_{\mathrm{op}}\left[\hat{\varphi}(1+2\boldsymbol{s}\cdot\hat{\boldsymbol{S}})-\hat{\rho}\right] =& R_{\mathrm{op}}\left[\hat{\boldsymbol{S}}\cdot\hat{\rho}\hat{\boldsymbol{S}}-\frac{3}{4}\hat{\rho}\right]+\frac{R_{\mathrm{op}}}{2}\left[\{\rho,S_z\}+(S_+\rho S_- - S_-\rho S_+)\right] \\ =& R_{\mathrm{op}}\left[S_z\rho S_z^\dagger-\frac{\{\rho,S_z^\dagger S_z\}}{2}+\frac{S_+\rho S_+^\dagger}{2}-\frac{\left\{\rho,S_+^\dagger S_+\right\}}{4}\right] \end{aligned} \tag{S5}$$

For spin-exchange interactions, it has been shown by K. Mouloudakis [2] that spin-exchange interactions can be written in Lindblad form by spin-exchange operator $\hat{P}_e = \mathcal{I}/2 + 2\langle\boldsymbol{S}\rangle\cdot\hat{\boldsymbol{S}}$,

$$R_{\mathrm{se}}\left[\hat{\varphi}\left(\mathcal{I}+4\langle\boldsymbol{S}\rangle\cdot\hat{\boldsymbol{S}}\right)-\hat{\rho}\right] = R_{\mathrm{se}}\left[\hat{P}_e\rho\hat{P}_e^\dagger-\frac{\left\{\hat{P}_e^\dagger\hat{P}_e,\hat{\rho}\right\}}{2}\right] \tag{S6}$$

Substitute Eq. (S3), Eq. (S5), and Eq. (S6) into Eq. (S1), we arrive at

$$\frac{\mathrm{d}\hat{\rho}}{\mathrm{d}t} = -\frac{i}{\hbar}\left[\hat{\mathcal{H}}_0,\hat{\rho}\right]+(R_{\mathrm{op}}+R_{\mathrm{sd}})\left[\hat{S}_z\hat{\rho}\hat{S}_z^\dagger-\frac{\left\{\hat{S}_z^\dagger\hat{S}_z,\hat{\rho}\right\}}{2}\right]+\frac{R_{\mathrm{op}}+R_{\mathrm{sd}}}{2}\left[\hat{S}_+\hat{\rho}\hat{S}_+^\dagger-\frac{\left\{\hat{S}_+^\dagger\hat{S}_+,\hat{\rho}\right\}}{2}\right] \tag{S7}$$

$$+\frac{R_{\mathrm{sd}}}{2}\left[\hat{S}_-\hat{\rho}\hat{S}_-^\dagger-\frac{\left\{\hat{S}_-^\dagger\hat{S}_-,\hat{\rho}\right\}}{2}\right]+R_{\mathrm{se}}\left[\hat{P}_e\rho\hat{P}_e^\dagger-\frac{\left\{\hat{P}_e^\dagger\hat{P}_e,\hat{\rho}\right\}}{2}\right]. \tag{S8}$$

By denoting

$$\hat{\mathcal{L}}_1 = \sqrt{R_{\mathrm{op}}+R_{\mathrm{sd}}}S_z, \tag{S9}$$

$$\hat{\mathcal{L}}_2 = \sqrt{\frac{R_{\mathrm{op}}+R_{\mathrm{sd}}}{2}}S_+, \tag{S10}$$

$$\hat{\mathcal{L}}_3 = \sqrt{\frac{R_{\mathrm{sd}}}{2}}S_-, \tag{S11}$$

$$\hat{\mathcal{L}}_4 = \sqrt{R_{\mathrm{se}}}P_e, \tag{S12}$$

the Eq. (S8) can be written as

$$\frac{\mathrm{d}\hat{\rho}}{\mathrm{d}t} = -\frac{i}{\hbar}\left[\hat{\mathcal{H}}_0,\hat{\rho}\right]+\sum_{i=1}^{4}\mathcal{L}_i\rho\mathcal{L}_i^\dagger-\frac{\{\mathcal{L}_i^\dagger\mathcal{L}_i,\rho\}}{2}, \tag{S13}$$

which gives the Eq. (1) in the manuscript.

II. BLOCH EQUATIONS IN EQUILIBRIUM LIMITS

Typically, when the Hamiltonian is axial-symmetric about $\hat{z}$-axis, the expectation value for z-component of the spin $\langle\hat{S}_z\rangle$ is conserved, which gives the so called spin-temperature distribution [1]. In statistical physics, when a system's total energy is fixed and the number of energy levels is constant, the populations of each energy level must follow a specific distribution if there are conservation laws related to the population numbers as constraints. Similarly, the essence of the spin-temperature distribution lies in the population distribution of the system under the constraints of particle number conservation and spin z-component conservation, when the system's density matrix maximizes entropy due to thermal equilibrium. This can be modeled by

$$\begin{aligned} \max \quad & \mathcal{S} = -\mathrm{Tr}[\hat{\rho}\ln\hat{\rho}], \\ \text{s.t.} \quad & 1 = \mathrm{Tr}[\hat{\rho}], \\ & \langle J_z\rangle = \mathrm{Tr}[\hat{\rho}\hat{J}_z]. \end{aligned} \tag{S14}$$

where $\mathcal{S}$ is density entropy. J is arbitrary angular momentum number. $\langle J_z\rangle$ is the z-component expected value for angular momentum $\boldsymbol{J}$, where $J = F, I, S$ can be total angular momentum F, nuclear spin I, or electronic spin S for alkali atoms. The optimization problem mentioned above can be formulated using the Lagrange multiplier method to derive the optimal equations

$$\frac{\partial f}{\partial \rho_i} = 0, \tag{S15}$$

where $f = \mathcal{S} + \alpha + \beta\langle J_z\rangle$ is the Lagrange function with α and β being Lagrangian constants, and ρ_i being the i-th diagonal element for density matrix $\hat{\rho}$. Then by solving the equation above, we can simply find $\rho_i \propto e^{\beta m_i}$. Therefore, the partition function can be expressed as

$$Z(J,\beta) = \frac{e^{\beta m_i}}{\sum_{i=1}^{2J+1} e^{\beta m_i}} = \frac{\sinh\left[\frac{\beta}{2}(2J+1)\right]}{\sinh\frac{\beta}{2}}, \tag{S16}$$

so that one can easily obtain

$$\langle J_z\rangle = \frac{d\ln Z}{d\beta} = \frac{1}{2}\varepsilon(J,\beta)\tanh\frac{\beta}{2}, \tag{S17}$$

where

$$\varepsilon(J,\beta) = (2J+1)\coth\left[\beta\left(J+\frac{1}{2}\right)\right]\coth\frac{\beta}{2} - \coth^2\frac{\beta}{2} = \langle J(J+1) - J_z^2\rangle. \tag{S18}$$

Thus, a slowing down factor q for Larmor frequency is introduced by considering the strong-coupling of hyperfine interaction

$$q = \frac{\langle F_z\rangle}{\langle S_z\rangle} = 1 + \varepsilon(I,\beta) \approx \frac{\langle F_i\rangle}{\langle S_i\rangle}, \quad i = x, y, z \tag{S19}$$

with $I = 3/2$ for ^{87}Rb. Eq. (S19) is the most important relationship for spin equilibrium temperature distribution which is usually written as $\langle \boldsymbol{F}\rangle = q\langle \boldsymbol{S}\rangle$.

On the other hand, we can turn density matrix evolution into the evolution of the expectation values for spin $\langle \boldsymbol{S}\rangle$ by multiplying Eq. (S1) with total angular momentum of alkali atom $\mathbf{F}$ and taking the trace, then we obtain

$$\frac{\partial\langle \boldsymbol{F}\rangle}{\partial t} = \gamma_e \boldsymbol{B}\times\langle \boldsymbol{S}\rangle + R_{\mathrm{op}}\left(\frac{1}{2}\boldsymbol{s} - \langle \boldsymbol{S}\rangle\right) - R_{\mathrm{sd}}\langle \boldsymbol{S}\rangle, \tag{S20}$$

where $\gamma_e = g_s\mu_B/\hbar$ is the electronic gyromagnetic ratio. With the spin equilibrium temperature distribution relationship from Eq. (S19) $\langle \boldsymbol{F}\rangle = q\langle \boldsymbol{S}\rangle$, we find the Bloch equation

$$\frac{\partial\langle \boldsymbol{S}\rangle}{\partial t} = \frac{\gamma_e}{q}\boldsymbol{B}\times\langle \boldsymbol{S}\rangle + \frac{R_{\mathrm{op}}}{q}\left(\frac{1}{2}\boldsymbol{s} - \langle \boldsymbol{S}\rangle\right) - \frac{R_{\mathrm{sd}}}{q}\langle \boldsymbol{S}\rangle, \tag{S21}$$

which is the original equation for alkali atomic spin ensemble given by Romalis [1, 3, 4].

III. SIMPLIFIED MODEL FOR THE EVOLUTION OF SPIN $\langle S\rangle$ UNDER FEEDBACK

In component form, the Eq. (S21) can be written as

$$\dot{S}_x = \frac{\gamma_e}{q}(B_y S_z - B_z S_y) - \frac{S_x}{T_2}, \tag{S22}$$

$$\dot{S}_y = \frac{\gamma_e}{q}(B_z S_x - B_x S_z) - \frac{S_y}{T_2}, \tag{S23}$$

$$\dot{S}_z = \frac{\gamma_e}{q}(B_x S_y - B_y S_x) - \frac{S_z}{T_2} + \frac{R_p}{2q}. \tag{S24}$$

where we have omit $\langle\rangle$ for simplification. But one should keep in mind that the S_i is an expectation value rather than an operator. $1/T_2 = (R_{\rm op} + R_{\rm sd})/q$ is the transverse relaxation rate. We consider the case that the magnetic field is $\boldsymbol{B} = (k_1 S_x^3 + k_2 \dot{S}_x, B_m \cos\omega_m t, B_0)$, then we have

$$\dot{S}_x = \omega_y S_z \cos\omega_m t - \omega_0 S_y - \frac{S_x}{T_2}, \tag{S25}$$

$$\dot{S}_y = \omega_0 S_x - \frac{\gamma_e}{q}(k_1 S_x^3 + k_2 \dot{S}_x) S_z - \frac{S_y}{T_2}, \tag{S26}$$

$$\dot{S}_z = \frac{\gamma_e}{q}\left(k_1 S_x^3 + k_2 \dot{S}_x\right) S_y - \omega_y \cos\omega_m t S_x - \frac{S_z}{T_2} + \frac{R_p}{2q}. \tag{S27}$$

where $\omega_0 = \gamma_e B_z/q, \omega_y = \gamma_e B_m/q$. Taking the derivative on both sides of Eq. (S25), we obtain

$$\ddot{S}_x + \frac{1}{T_2}\dot{S}_x = -\omega_0 \dot{S}_y - \omega_y \omega_m S_z \sin\omega_m t + \omega_y \dot{S}_z \cos\omega_m t. \tag{S28}$$

Substitute Eq. (S26) into Eq. (S31), we find

$$\ddot{S}_x + \left(\frac{1}{T_2} - k_2 \frac{\gamma_e}{q}\omega_0 S_z\right)\dot{S}_x + \omega_0^2 S_x - k_1 \frac{\gamma_e}{q}\omega_0 S_z S_x^3 = \frac{\omega_0}{T_2} S_y - \omega_y \omega_m S_z \sin\omega_m t + \omega_y \dot{S}_z \cos\omega_m t. \tag{S29}$$

According to Eq. (S25), we have

$$S_y = -\frac{1}{\omega_0}\left(\dot{S}_x + \frac{1}{T_2} S_x - \omega_y S_z \cos\omega_m t\right). \tag{S30}$$

Substitute Eq. (S30) into Eq. (S31), then we find

$$\ddot{S}_x + \left(\frac{2}{T_2} - k_2 \frac{\gamma_e}{q}\omega_0 S_z\right)\dot{S}_x + \left(\omega_0^2 + \frac{1}{T_2^2}\right) S_x - k_1 \frac{\gamma_e}{q}\omega_0 S_z S_x^3 = \Omega_m S_z \left(\frac{1}{T_2}\cos\omega_m t - \omega_m \sin\omega_m t\right) + \omega_y \dot{S}_z \cos\omega_m t. \tag{S31}$$

In our simplified model, we take the longitude spin to be steady, i.e., $\dot{S}_z = 0$, to find that $S_z = S_0 = R_p T_2/2q$ is a constant which is usually used in most of the analysis for spin dynamics. This assumption is well satisfied when the Larmor frequency induced by transverse magnetic field is much smaller than pumping rate, i.e., $\gamma|B_\perp| \ll R_p$. Then we find the equation above can be written as

$$\ddot{S}_x + \Gamma \dot{S}_x + \alpha S_x + \beta S_x^3 = A\cos(\omega_m t + \phi). \tag{S32}$$

where

$$\Gamma = \frac{2}{T_2} - k_2 \frac{\gamma_e}{q}\omega_0 S_0, \tag{S33}$$

$$\alpha = \omega_0^2 + \frac{1}{T_2^2}, \tag{S34}$$

$$\beta = -k_1 \frac{\gamma_e}{q}\omega_0 S_0, \tag{S35}$$

$$A = \omega_y S_z \sqrt{\frac{1}{T_2^2} + \omega_m^2}, \tag{S36}$$

$$\phi = \frac{\omega_m}{T_2}. \tag{S37}$$

The Eq. (S32) is the so-called Duffing oscillator model for the Eq.(2) in the manuscript, which is a fundamental model in chaos generation. In the process of chaotic generation within the Duffing system, two essential conditions must be satisfied: (1) sufficiently strong nonlinearity and (2) adequately long coherence time to sustain chaotic dynamics. Phenomenologically, the cubic feedback proportional to k_1 totally determine the nonlinear term, which is responsible for generating chaos. The derivative feedback proportional to k_2 therefore serves to adjust the effective coherence time γ through parametric control. In our experiments, though we set $\omega_m = 0$, negative Γ is realized by tuning k_2. This drives the system into a self-sustained oscillation phase which can also generate chaotic behavior.

IV. SELF-SUSTAINED OSCILLATION BY DERIVATIVE FEEDBACK

We will demonstrate the origin of self oscillation by derivative feedback. Now consider the stability of the equations Eq. (S22)-Eq. (S24) when there is ONLY derivative feedback term $k_2\dot{S}_x$, which gives

$$\dot{S}_x = \frac{\gamma_e}{q}\left(B_y S_z - B_z S_y\right) - \frac{S_x}{T_2}, \tag{S38}$$

$$\dot{S}_y = \frac{\gamma_e}{q}\left(B_z S_x - k_2 \dot{S}_x S_z\right) - \frac{S_y}{T_2}, \tag{S39}$$

$$\dot{S}_z = \frac{\gamma_e}{q}\left(k_2 \dot{S}_x S_y - B_y S_x\right) - \frac{S_z}{T_2} + \frac{R_p}{2}. \tag{S40}$$

Substituting Eq. (S38) into Eq. (S39) and Eq. (S40), we find

$$\dot{S}_x = \frac{\gamma_e}{q}\left(B_y S_z - B_z S_y\right) - \frac{S_x}{T_2}, \tag{S41}$$

$$\dot{S}_y = \frac{\gamma_e}{q} B_z S_x - k_2 \frac{\gamma_e^2}{q^2} B_y S_z^2 + k_2 \frac{\gamma_e^2}{q^2} B_z S_y S_z + k_2 \frac{\gamma_e}{q}\frac{S_x S_z}{T_2} - \frac{S_y}{T_2}, \tag{S42}$$

$$\dot{S}_z = k_2 \frac{\gamma_e^2}{q^2} B_y S_y S_z - k_2 \frac{\gamma_e^2}{q^2} B_z S_y^2 - k_2 \frac{\gamma_e}{q}\frac{S_x S_y}{T_2} - \frac{\gamma_e}{q} B_y S_x - \frac{S_z}{T_2} + \frac{R_p}{2}. \tag{S43}$$

We linearize these equation around the equilibrium point by $\boldsymbol{S} = \boldsymbol{S}^* + \delta\boldsymbol{S}$ where the equilibrium point $\boldsymbol{S}^*$ is given by $\dot{\boldsymbol{S}} = 0$ with perturbation $\delta\boldsymbol{S}$. The complete steady solution for these equations has been given by Seltzer [5]. For simplicity, one can directly set $S_x^* = S_y^* = 0$, $S_z^* = R_p T_2/2 = S_0$ for a good approximation around the real equilibrium point. Then we have $S_x = \delta S_x, S_y = \delta S_y, S_z = S_0 + \delta S_z$. Noting the definition of $\boldsymbol{S}^*$ and neglecting the second order term in $\delta S_i \delta S_j, i, j = x, y, z$, the equations above can be simplified to

$$\delta\dot{S}_x = -\frac{\delta S_x}{T_2} - \frac{\gamma_e}{q} B_z \delta S_y + \frac{\gamma_e}{q} B_y \delta S_z, \tag{S44}$$

$$\delta\dot{S}_y = \left(\frac{\gamma_e}{q} B_z + k_2 \frac{\gamma_e}{q}\frac{S_0}{T_2}\right)\delta S_x + \left(k_2 \frac{\gamma_e^2}{q^2} B_z S_0 - \frac{1}{T_2}\right)\delta S_y - 2k_2 \frac{\gamma_e^2}{q^2} B_y S_0 \delta S_z, \tag{S45}$$

$$\delta\dot{S}_z = -\frac{\gamma_e}{q} B_y \delta S_x + k_2 \frac{\gamma_e^2}{q^2} B_y S_0 \delta S_y - \frac{\delta S_z}{T_2}. \tag{S46}$$

These equations can be written in matrix form,

$$\frac{\mathrm{d}}{\mathrm{d}t}|\psi\rangle = \begin{pmatrix} \delta\dot{S}_x \\ \delta\dot{S}_y \\ \delta\dot{S}_z \end{pmatrix} = -i \begin{pmatrix} -i\frac{1}{T_2} & -i\frac{\gamma_e}{q} B_z & i\frac{\gamma_e}{q} B_y \\ i\frac{\gamma_e}{q} B_z + ik_2 \frac{\gamma_e}{q}\frac{S_0}{T_2} & ik_2 \frac{\gamma_e^2}{q^2} B_z S_0 - i\frac{1}{T_2} & -2ik_2 \frac{\gamma_e^2}{q^2} B_y S_0 \\ -i\frac{\gamma_e}{q} B_y & ik_2 \frac{\gamma_e^2}{q^2} B_y S_0 & -i\frac{1}{T_2} \end{pmatrix} \begin{pmatrix} \delta S_x \\ \delta S_y \\ \delta S_z \end{pmatrix} = -i\mathcal{H}_{\text{eff}}|\psi\rangle \tag{S47}$$

where $|\psi\rangle = [\delta S_x, \delta S_y, \delta S_z]^T$ is an effective state vector combined by each component of perturbation $\delta\boldsymbol{S}$. In this way, we formally obtain an effective non-Hermitian Hamiltonian $\mathcal{H}_{\text{eff}}$ for perturbation so that quantum theory can be applied to this effective system as shown in Eq. (3) in the manuscript. We calculate the eigenvalues $\lambda = \omega + i\Gamma$ for the effective Hamiltonian $\mathcal{H}_{\text{eff}}$ by varying k_2 as shown in FIG. (3) (a) in the manuscript.

It can be shown that the evolution for $\psi\rangle$ is proportional to $e^{\lambda t} = e^{\Gamma t} e^{-i\omega t}$. When $k_2 = 0$, the system has the relaxation rate $1/T_2 = 20\text{Hz}$ while the evolution frequency $\omega/2\pi = 84.6\,\text{Hz}$ given by magnetic field $|B| = 15.5\text{nT}$. Interestingly, we find exceptional points(EP) typically appeared in non-Hermitian physics. However, in experiments, the large k_2 regime has no signal since the Larmor frequency is zero, making this result trivial. The main point in this work lies in the regime where $k_2 \in [0.005, 0.239]$ (red lines). In this regime, both of the eigenvalues for S_x and S_y are degenerated and have positive real part $\Gamma > 0$ while the imaginary part is non-zero, corresponding to gain in amplitude and oscillation in phase. This is the essential point for generating self oscillation. The typical behavior for this phenomenon is that the amplitude grows rapidly with oscillation. However, this model is effective only when the spin is near equilibrium point S^* since the amplitude of $\delta S_{x/y}$ will be infinity when $t \to +\infty$. Thus, this model describes whether the amplitude of a small perturbation will grow or damp, and also the phase of a small perturbation will oscillate or not. This is an intuitive explain for the origin of self-oscillation by derivative feedback. For further accurate understanding when the spin is far from the equilibrium point, it can be fully but numerically analyzed by density matrix.

V. DETAILED MODEL FOR NUMERICALLY ANALYZING SPIN DYNAMICS

Though Eq. (S32) is a simple model for explaining the fact that this system can generate chaos, we have to confess that there is one serious problem in this model. In spin equilibrium temperature distribution regime induced by frequency spin exchange collisions between alkali atoms, one can obtain the relationship between atomic spin $\boldsymbol{F}$ and electronic spin $\boldsymbol{S}$ satisfy $\boldsymbol{F} = q\boldsymbol{S}$ by maximizing the spin entropy $\mathcal{S} = -\rho \ln \rho$ under the restriction condition of spin number conservation $\mathrm{Tr}[\rho] = 1$ and longitudinal spin component conservation $S_z = S_0$. In this sense, this result can only be reached when longitudinal spin S_z is a constant, or equivalently, $\dot{S}_z = 0$. We also utilize this assumption in deriving Eq. (S32) from Eq. (S31). Take these facts into consideration, Bloch equations for electronic spin Eq. (S22)-Eq. (S24) are no more accurate description for spin dynamics unless a time dependence is considered in q.

To address the problems above, we perform our analysis based on density matrix. The density matrix is given by Eq. (1) in the main text. We solve the density matrix in coupled representation $|F, m_F\rangle$, which is the eigenstates for hyperfine interactions $A_{\mathrm{hfs}}\hat{\boldsymbol{I}} \cdot \hat{\boldsymbol{S}}$, but not for Zeeman interaction whose eigenstates are uncoupled basis $|m_I, m_S\rangle = |I, m_I\rangle \otimes |S, m_S\rangle$. This means we need to express all the operators in the coupled representation. This process can be achieved through a change of representation for operators from uncoupled basis $\hat{\mathcal{O}}_{\mathrm{UC}}$ to coupled basis by $\hat{\mathcal{O}} = U\hat{\mathcal{O}}_{\mathrm{UC}}U^{\dagger}$given by the unitary transformation,

$$|m_I, m_S\rangle = \sum_{F,mF} |F, m_F\rangle\langle F, m_F|m_I, m_S\rangle = U|F, m_F\rangle. \tag{S48}$$

For ^{87}Rb, electronic spin $S = 1/2$, nuclear spin $I = 3/2$, atomic spin $F = I \pm S = 1, 2$. The basis order is defined by

$$|\Psi\rangle = [|2, +2\rangle, |2, +1\rangle, ..., |2, -2\rangle, |1, +1\rangle, |1, 0\rangle, |1, -1\rangle]^T \tag{S49}$$

For completeness, we directly list the matrix form for all the operators in our simulation in coupled basis. For ^{87}Rb, $I = 3/2, F = 1, 2$, we find unitary transform matrix

$$U = \begin{pmatrix} 1 & 0 & 0 & 0 & 0 & 0 & 0 & 0 \\ 0 & \frac{1}{2} & 0 & 0 & 0 & \frac{\sqrt{3}}{2} & 0 & 0 \\ 0 & \frac{\sqrt{3}}{2} & 0 & 0 & 0 & -\frac{1}{2} & 0 & 0 \\ 0 & 0 & \frac{\sqrt{2}}{2} & 0 & 0 & 0 & \frac{\sqrt{2}}{2} & 0 \\ 0 & 0 & \frac{\sqrt{2}}{2} & 0 & 0 & 0 & -\frac{\sqrt{2}}{2} & 0 \\ 0 & 0 & 0 & \frac{\sqrt{3}}{2} & 0 & 0 & 0 & \frac{1}{2} \\ 0 & 0 & 0 & \frac{1}{2} & 0 & 0 & 0 & -\frac{\sqrt{3}}{2} \\ 0 & 0 & 0 & 0 & 1 & 0 & 0 & 0 \end{pmatrix}, \tag{S50}$$

and the spin operators

$$\hat{S}_+ = \begin{pmatrix} 0 & \frac{1}{2} & 0 & 0 & 0 & \frac{\sqrt{3}}{2} & 0 & 0 \\ 0 & 0 & \frac{\sqrt{6}}{4} & 0 & 0 & 0 & \frac{\sqrt{6}}{4} & 0 \\ 0 & 0 & 0 & \frac{\sqrt{6}}{4} & 0 & 0 & 0 & \frac{\sqrt{2}}{4} \\ 0 & 0 & 0 & 0 & \frac{1}{2} & 0 & 0 & 0 \\ 0 & 0 & 0 & 0 & 0 & 0 & 0 & 0 \\ 0 & 0 & -\frac{\sqrt{2}}{4} & 0 & 0 & 0 & -\frac{\sqrt{2}}{4} & 0 \\ 0 & 0 & 0 & -\frac{\sqrt{6}}{4} & 0 & 0 & 0 & -\frac{\sqrt{2}}{4} \\ 0 & 0 & 0 & 0 & -\frac{\sqrt{3}}{2} & 0 & 0 & 0 \end{pmatrix}, \hat{S}_- = \begin{pmatrix} 0 & 0 & 0 & 0 & 0 & 0 & 0 & 0 \\ \frac{1}{2} & 0 & 0 & 0 & 0 & 0 & 0 & 0 \\ 0 & \frac{\sqrt{6}}{4} & 0 & 0 & 0 & -\frac{\sqrt{2}}{4} & 0 & 0 \\ 0 & 0 & \frac{\sqrt{6}}{4} & 0 & 0 & 0 & -\frac{\sqrt{6}}{4} & 0 \\ 0 & 0 & 0 & \frac{1}{2} & 0 & 0 & 0 & -\frac{\sqrt{3}}{2} \\ \frac{\sqrt{3}}{2} & 0 & 0 & 0 & 0 & 0 & 0 & 0 \\ 0 & \frac{\sqrt{6}}{4} & 0 & 0 & -\frac{\sqrt{2}}{4} & 0 & 0 & 0 \\ 0 & 0 & \frac{\sqrt{2}}{4} & 0 & 0 & 0 & -\frac{\sqrt{2}}{4} & 0 \end{pmatrix},$$

$$\hat{I}_+ = \begin{pmatrix} 0 & \frac{3}{2} & 0 & 0 & 0 & -\frac{\sqrt{3}}{2} & 0 & 0 \\ 0 & 0 & \frac{3\sqrt{6}}{4} & 0 & 0 & 0 & -\frac{\sqrt{6}}{4} & 0 \\ 0 & 0 & 0 & \frac{3\sqrt{6}}{4} & 0 & 0 & 0 & -\frac{\sqrt{2}}{4} \\ 0 & 0 & 0 & 0 & \frac{3}{2} & 0 & 0 & 0 \\ 0 & 0 & 0 & 0 & 0 & 0 & 0 & 0 \\ 0 & 0 & \frac{\sqrt{2}}{4} & 0 & 0 & 0 & \frac{5\sqrt{2}}{4} & 0 \\ 0 & 0 & 0 & \frac{\sqrt{6}}{4} & 0 & 0 & 0 & \frac{5\sqrt{2}}{4} \\ 0 & 0 & 0 & 0 & \frac{\sqrt{3}}{2} & 0 & 0 & 0 \end{pmatrix}, \hat{I}_- = \begin{pmatrix} 0 & 0 & 0 & 0 & 0 & 0 & 0 & 0 \\ \frac{3}{2} & 0 & 0 & 0 & 0 & 0 & 0 & 0 \\ 0 & \frac{3\sqrt{6}}{4} & 0 & 0 & 0 & \frac{\sqrt{2}}{4} & 0 & 0 \\ 0 & 0 & \frac{3\sqrt{6}}{4} & 0 & 0 & 0 & \frac{\sqrt{6}}{4} & 0 \\ 0 & 0 & 0 & \frac{3}{2} & 0 & 0 & 0 & \frac{\sqrt{3}}{2} \\ -\frac{\sqrt{3}}{2} & 0 & 0 & 0 & 0 & 0 & 0 & 0 \\ 0 & -\frac{\sqrt{6}}{4} & 0 & 0 & 0 & \frac{5\sqrt{2}}{4} & 0 & 0 \\ 0 & 0 & -\frac{\sqrt{2}}{4} & 0 & 0 & 0 & \frac{5\sqrt{2}}{4} & 0 \end{pmatrix},$$

$$\hat{S}_z = \begin{pmatrix} \frac{1}{2} & 0 & 0 & 0 & 0 & 0 & 0 & 0 \\ 0 & \frac{1}{4} & 0 & 0 & 0 & -\frac{\sqrt{3}}{4} & 0 & 0 \\ 0 & 0 & 0 & 0 & 0 & 0 & -\frac{1}{2} & 0 \\ 0 & 0 & 0 & -\frac{1}{4} & 0 & 0 & 0 & -\frac{\sqrt{3}}{4} \\ 0 & 0 & 0 & 0 & -\frac{1}{2} & 0 & 0 & 0 \\ 0 & -\frac{\sqrt{3}}{4} & 0 & 0 & 0 & -\frac{1}{4} & 0 & 0 \\ 0 & 0 & -\frac{1}{2} & 0 & 0 & 0 & 0 & 0 \\ 0 & 0 & 0 & -\frac{\sqrt{3}}{4} & 0 & 0 & 0 & \frac{1}{4} \end{pmatrix}, \hat{I}_z = \begin{pmatrix} \frac{3}{2} & 0 & 0 & 0 & 0 & 0 & 0 & 0 \\ 0 & \frac{3}{4} & 0 & 0 & 0 & \frac{\sqrt{3}}{4} & 0 & 0 \\ 0 & 0 & 0 & 0 & 0 & 0 & \frac{1}{2} & 0 \\ 0 & 0 & 0 & -\frac{3}{4} & 0 & 0 & 0 & \frac{\sqrt{3}}{4} \\ 0 & 0 & 0 & 0 & -\frac{3}{2} & 0 & 0 & 0 \\ 0 & \frac{\sqrt{3}}{4} & 0 & 0 & 0 & \frac{5}{4} & 0 & 0 \\ 0 & 0 & \frac{1}{2} & 0 & 0 & 0 & 0 & 0 \\ 0 & 0 & 0 & \frac{\sqrt{3}}{4} & 0 & 0 & 0 & -\frac{5}{4} \end{pmatrix}.$$

For atomic spin operators, we calculate from the eigenvalue directly under coupled basis by $\hat{F}_z|F, m_F\rangle = m_F|F, m_F\rangle$ and $\hat{F}_\pm|F, m_F\rangle = \sqrt{F(F+1) - m_F(m_F \pm 1)}|F, m_F\rangle$ to find

$$\hat{F}_+ = \begin{pmatrix} 0 & 2 & 0 & 0 & 0 & 0 & 0 & 0 \\ 0 & 0 & \sqrt{6} & 0 & 0 & 0 & 0 & 0 \\ 0 & 0 & 0 & \sqrt{6} & 0 & 0 & 0 & 0 \\ 0 & 0 & 0 & 0 & 2 & 0 & 0 & 0 \\ 0 & 0 & 0 & 0 & 0 & 0 & 0 & 0 \\ 0 & 0 & 0 & 0 & 0 & 0 & \sqrt{2} & 0 \\ 0 & 0 & 0 & 0 & 0 & 0 & 0 & \sqrt{2} \\ 0 & 0 & 0 & 0 & 0 & 0 & 0 & 0 \end{pmatrix}, \hat{F}_- = \begin{pmatrix} 0 & 0 & 0 & 0 & 0 & 0 & 0 & 0 \\ 2 & 0 & 0 & 0 & 0 & 0 & 0 & 0 \\ 0 & \sqrt{6} & 0 & 0 & 0 & 0 & 0 & 0 \\ 0 & 0 & \sqrt{6} & 0 & 0 & 0 & 0 & 0 \\ 0 & 0 & 0 & 2 & 0 & 0 & 0 & 0 \\ 0 & 0 & 0 & 0 & 0 & 0 & 0 & 0 \\ 0 & 0 & 0 & 0 & 0 & \sqrt{2} & 0 & 0 \\ 0 & 0 & 0 & 0 & 0 & 0 & \sqrt{2} & 0 \end{pmatrix}, \hat{F}_z = \begin{pmatrix} 2 & 0 & 0 & 0 & 0 & 0 & 0 & 0 \\ 0 & 1 & 0 & 0 & 0 & 0 & 0 & 0 \\ 0 & 0 & 0 & 0 & 0 & 0 & 0 & 0 \\ 0 & 0 & 0 & -1 & 0 & 0 & 0 & 0 \\ 0 & 0 & 0 & 0 & -2 & 0 & 0 & 0 \\ 0 & 0 & 0 & 0 & 0 & 1 & 0 & 0 \\ 0 & 0 & 0 & 0 & 0 & 0 & 0 & 0 \\ 0 & 0 & 0 & 0 & 0 & 0 & 0 & -1 \end{pmatrix}.$$

With these matrix, we are able to numerically solve Eq. (S1) by 4th order Runge-Kutta method. One can verify these operators by the relationship $\hat{F}_i = \hat{I}_i + \hat{S}_i, i = x, y, z, \pm$. We list $\hat{F}_i$ operators to numerically show that when S_z can no more be regarded a constant, and how accuracy Bloch equations are by setting q as a constant. We also calculate the slowing down factor according to the original definition $q = \langle F_z\rangle/\langle S_z\rangle$ with $\langle F_z\rangle = \mathrm{Tr}[\hat{\rho}\hat{F}_z]$ and $\langle S_z\rangle = \mathrm{Tr}[\hat{\rho}\hat{S}_z]$ obtained from density matrix to evaluate whether the spin in our experiment is in a non-equilibrium case. Through

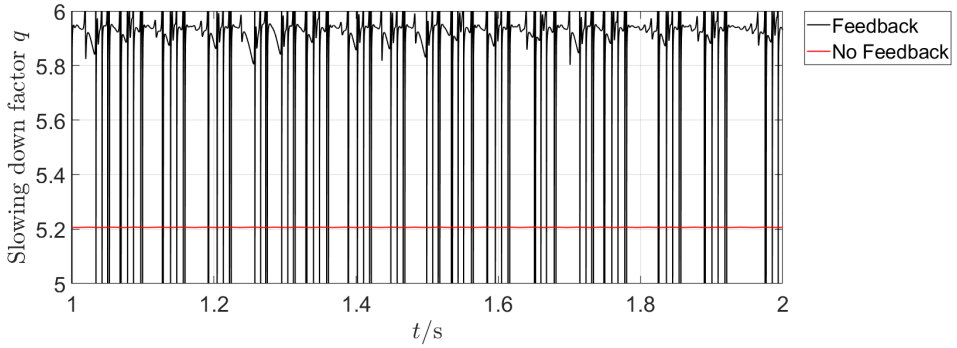

FIG. S1. Slowing down factor q calculated by original definition in [1] using density matrix. When there is no feedback, the time evolution of q can be regarded as a constant in red line, while this result can be broken when feedback is added as given by the black line. This result can be much larger or even negative than the theoretical boundary for $q \in [4, 6]$ in equilibrium state, showing the evidence for the system to go into non-equilibrium state. The feedback parameters are $k_1 = 1.5 \times 10^5$ and $k_2 = 0.29$. The data for analysis is set to [1, 2] s to avoid numerical instability due to initial conditions in simulation. In simulation, $R_{\mathrm{sd}} = R_{\mathrm{op}} = 100\mathrm{s}^{-1}$, $T = 428.15\mathrm{K}$, $q = 5.2$.

numerical simulations of the density matrix Eq. (S1), we calculate the slowing down factor q corresponding to the spin equilibrium temperature distribution. Under our experimental configuration, this factor is defined as the ratio between the z-component of total atomic spin F_z and the electronic spin S_z for ^{87}Rb atoms, yielding a value of $q = (6 + 2P^2)/(1 + P^2) \in [4, 6]$ [1], where $P = \langle S_z\rangle/S$ is the spin polarization. In the absence of feedback, the polarization $P = 0.5$ corresponds to a slowing down factor of $q = 5.2$, as the red line shown in FIG. S1. Remarkably, when feedback is introduced, the slowing down factor exhibits oscillatory behavior. This parameter exceeds its original numerical range in spin equilibrium state and diverges at some points when S_z is near zero, thereby invalidating the Bloch equations derived from the spin equilibrium temperature distribution. This divergence provides indirect evidence that the system has been broken away from spin equilibrium. In this sense, we say that the system is in spin non-equilibrium state. The physical picture for this phenomenon is the large transverse feedback magnetic field flips the $\langle S_z\rangle$ from $+\hat{\boldsymbol{z}}$ to $-\hat{\boldsymbol{z}}$ direction, which will generate a point with $\langle S_z\rangle = 0$ while $\langle F_z\rangle \neq 0$ in turn making the ratio $q = \langle F_z\rangle/\langle S_z\rangle$ diverge around every zero point.

VI. ENCRYPTION PRINCIPLE AND EXAMPLE

To demonstrate the feasibility of encoding for this system, we set $k_2 = 0.24$ in the experiment to obtain the self-sustained frequency $\omega_0 = 2\pi \times 83.05\,\mathrm{Hz}$ by setting $B_z = 15.5\,\mathrm{nT}$. Then we apply a modulation magnetic field $\delta B_z \cos\omega_0 t$ in the z-axis so that the system can work in different phases when varying the amplitude of δB_z. As shown in FIG. S2, when the amplitude δB_z is small ($\leq 7.99\,\mathrm{nT}$), there is only one main peak in the PSD. Further increasing in δB_z produces unstable subharmonic components, which gradually converges to 1/2-subharmonics. There is a robust regime in $[10.75, 14.46]\,\mathrm{nT}$ where both the main peak and the 1/2-harmonics co-exist. Then, the system goes into a new unstable region from $14.46\,\mathrm{nT}$ to $15.69\,\mathrm{nT}$ with inverse Farey tree like structures. Interestingly, in $[15.69, 16.47]\,\mathrm{nT}$, the system, again, produce stable multi-subharmonics to 7-th order. If we define the 3 different phases as 3 different codes such as 0, 1, 2, then we are able to encode the signal by the PSD.

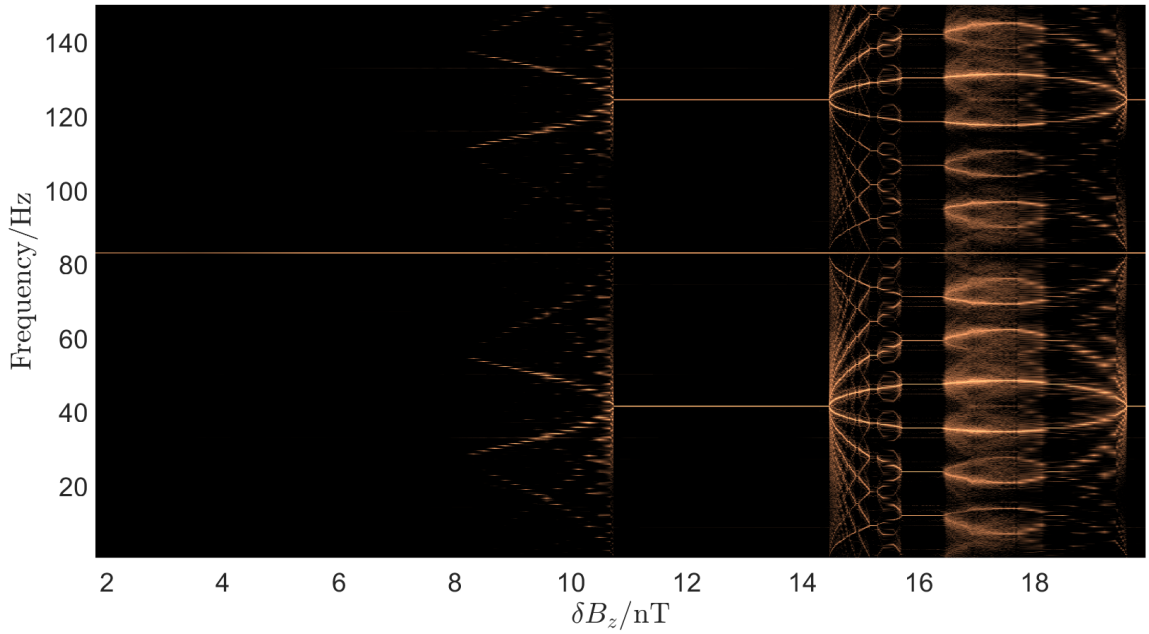

FIG. S2. Phase encoding verification. The feedback magnetic field is given by setting small cubic feedback $k_1 = 2000$ and proper $k_2 = 0.24$ to generate the self-sustained oscillation. Three distinct stable regimes are found in $[2, 7.99]\,\mathrm{nT}$, $[10.75, 14.46]\,\mathrm{nT}$, $[15.69, 16.47]\,\mathrm{nT}$. These three regimes can be noted as state 1, 2, 3, respectively. Other state can be obtained by setting larger δB_z. These states are robust to the noise when operating in the center of the regimes.

The encryption mechanism proposed herein exploits the phase-dependent chaotic dynamics of the thermal atomic spin ensemble, modulated by the amplitude of the magnetic field δB_z. The principle hinges on encoding information into distinct stable states of the power spectral density (PSD) by varying δB_z within specific amplitude ranges, each corresponding to a unique phase regime. These regimes—$[2, 7.99]$ nT (state 0, characterized by a single dominant peak), $[10.75, 14.46]$ nT (state 1, featuring coexisting main peak and 1/2-subharmonics), and $[15.69, 16.47]$ nT (state 2, exhibiting stable multi-subharmonics up to 7th order)—serve as the foundational encoding states, as demonstrated in FIG. S2. The chaotic behavior in the unstable region $[14.46, 15.69]$ nT, marked by inverse Farey tree structures, enhances security by introducing sensitivity to initial conditions and parameter perturbations. A dynamic phase modulation $\phi(t)$ is incorporated into the modulation field $\delta B_z \cos(\omega_0 t + \phi(t))$, where $\phi(t)$ acts as a time-varying encryption key. The encrypted signal is transmitted as the PSD, which is subsequently can be decoded using threshold pre-calibration by FFT or a machine learning method trained on experimental PSD data. The robustness of these states to noise, particularly at the centers of the stable regimes, ensures reliable signal integrity, while the complexity of the chaotic trajectories provides resistance against unauthorized decryption.

As a concrete example, consider the encryption of the binary message "101" using the defined states. The encoding process maps "1" to state 1 ($\delta B_z = 12.6$ nT, the center of $[10.75, 14.46]$ nT), "0" to state 0 ($\delta B_z = 5$ nT, within $[2, 7.99]$ nT), and "1" to state 1 ($\delta B_z = 12.6$ nT). The sender modulates the magnetic field as $\delta B_z(t) = \delta B_z^0 + \Delta B_z \cos(\omega_0 t + \phi(t))$, where δB_z^0 cycles through 5 nT, 12.6 nT, and 12.6 nT across corresponding time slots for each bit. The dynamic phase $\phi(t)$ is a pseudo-random sequence, e.g., $\phi(t) = 0.1 \times 2\pi t$, shared as the secret key with the receiver.

The resulting PSD is measured and transmitted: state 0 yields a single peak at $\omega_0 = 2\pi \times 83.05$ Hz, while state 1 produces a main peak with 1/2-subharmonics. The receiver, synchronized with the key $\phi(t)$ and the self-sustained frequency ω_0, employs the threshold detection or the pre-trained machine learning model to analyze the PSD features and reconstruct the sequence of states (0, 1, 1), decoding the original message "101". This example illustrates the efficacy of the proposed chaotic phase-encoding scheme for secure communication, leveraging the system's nonlinear dynamics and experimental robustness.

VII. ELECTRONIC CIRCUITS FOR FEEDBACK

The analog multiplier circuit is designed around the AD835 chip as shown in FIG. S3, a four-quadrant analog multiplier capable of performing multiplication of two input signals and producing an output proportional to their product. Input signals are fed into the X1 and Y1 pins of the AD835 via SMA connectors P2 and P4, respectively. The output signal is taken from the W pin of the AD835 and coupled through a 0.1 μF capacitor (C4) to an SMA connector P3 for AC coupling. The circuit operates with a dual power supply (VDD and VEE), with power stability ensured by filter capacitors C1, C2, C9, and C10 (0.1 μF and 1 μF) and filters F1 and F2, which effectively suppress noise interference. To optimize signal transmission, impedance matching is achieved using matching networks SB1, SB2, and SB3. The primary function of this circuit is to perform analog multiplication of two input signals, making

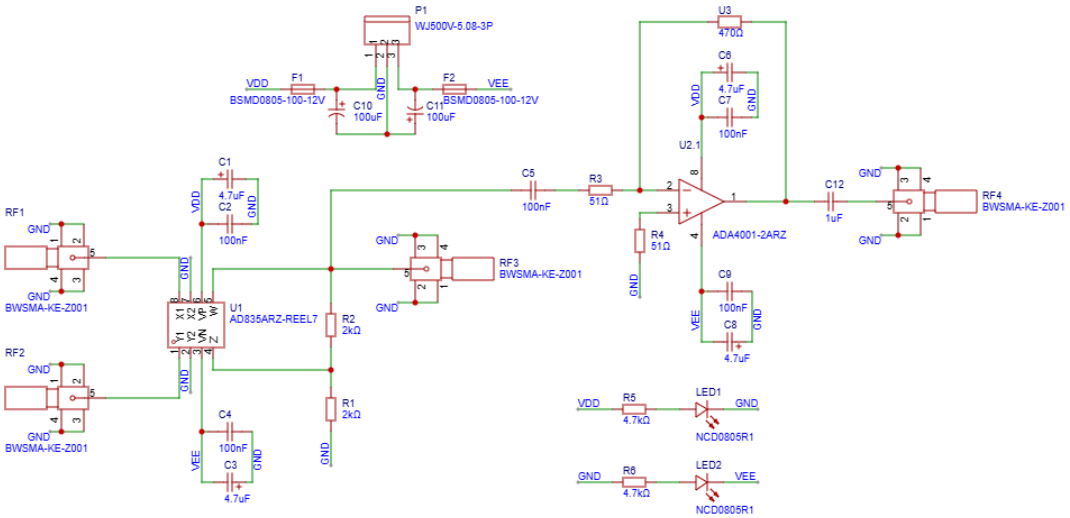

FIG. S3. Schematic for multiplier circuit.

it suitable for a wide range of signal processing applications. To achieve cubic multiplication of a signal, two of the above analog multiplier circuits are configured in a cascaded arrangement. The experimental setup splits an input signal $s \propto \langle S_x \rangle$ into three identical signals s_1, s_2, and s_3 using two three-way splitters. The first multiplier takes s_1 and s_2 as inputs, producing an output signal $s_4 = s_1 s_2$. Subsequently, the second multiplier multiplies s_3 with s_4, yielding the final output $s_5 = s_3 \times s_4 = s_3(s_1 s_2)$. Since $s_1 = s_2 = s_3 = s$, the final output becomes $s_{\text{out}} = s^3 \propto \langle S_x \rangle^3$, thus achieving the cubic multiplication for the feedback signal.

The derivative circuit is designed around the AD8421 chip as shown in FIG. S4, a high-performance instrumentation amplifier with low noise, high common-mode rejection ratio, and wide bandwidth (~10 MHz), making it ideal for high-precision differential signal processing. Input signals are fed into the IN+ and IN- pins of the AD8421 via SMA connectors P4 and P7, forming a differential input. The gain is set by an external resistor R2 (10 kΩ), with the gain formula $G = 1 + \frac{9.9\text{k}\Omega}{R_G}$, yielding $G \approx 1.99$. The output signal is taken from the OUT pin of the AD8421 and transmitted through an SMA connector P6. The circuit operates with a dual power supply (V+ and V-), with power stability ensured by filter capacitors C3, C9, C10, C11, and C12 (all 100 nF), reducing noise interference. The REF pin is grounded through a resistor R7 (100 Ω) and a capacitor C11 (100 nF) to set the output reference level. Additionally, an OPA177 operational amplifier (U2) is included, likely for generating a stable reference voltage.

The experimental setup realizes the derivative of the signal $\langle S_x \rangle$, denoted as $\langle \dot{S}_x \rangle$, using a difference approximation. The input signal $\langle S_x \rangle$ is split into two paths: one path, the current signal $\langle S_x(t) \rangle$, is fed into the IN+ pin of the AD8421, while the other path, a delayed signal $\langle S_x(t - \Delta t) \rangle$, is delayed by Δt and input to the IN- pin. The AD8421

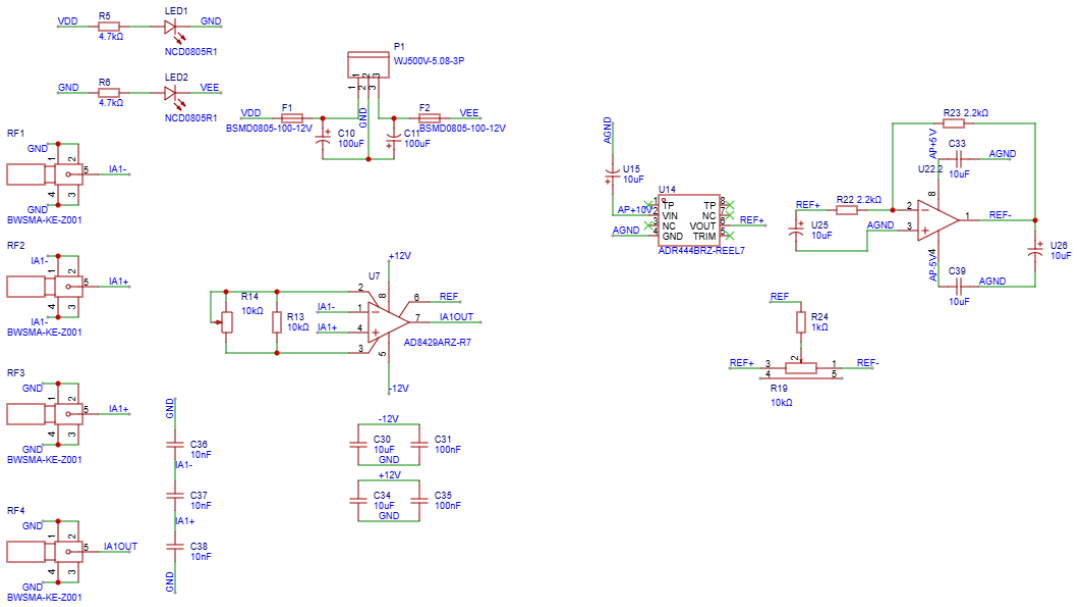

FIG. S4. Schematic for derivative circuit.

performs a differential operation, producing an output $V_{\text{out}} = G \cdot (\langle S_x(t) \rangle - \langle S_x(t - \Delta t) \rangle)$, where $G \approx 1.99$. Using the known time interval Δt, the difference approximates the derivative $\langle \dot{S}_x \rangle \approx \frac{\langle S_x(t) \rangle - \langle S_x(t-\Delta t) \rangle}{\Delta t}$. The final output V_{out} is extracted from P6, and by scaling with a factor of $\eta = G/\Delta t$, the derivative proportional to $\langle \dot{S}_x \rangle$ is obtained.

The experimental configuration connects the outputs of the AD835 and AD8421 to two separate variable feedback resistors (FRs) and feedback coils (FCs) to achieve experimentally adjustable gain. The gain G of the chips is determined by the feedback resistors FR1 and FR2. Adjusting the variable feedback resistors dynamically changes the FRs to tune the gain. The feedback coils feed the output signal back to the spin by magnetic field, further influencing the gain or the dynamic response of the signal. This feedback mechanism optimizes the gain for different signal amplitudes, enhancing the circuit's flexibility and applicability.

[1] S. Appelt, A. B.-A. Baranga, C. J. Erickson, M. V. Romalis, A. R. Young, et al., Theory of spin-exchange optical pumping of 3 He and 129 Xe, Physical Review A **58**, 1412 (1998).

[2] K. Mouloudakis, Spin noise correlations in multispecies hot atomic vapors, Ph.D. thesis, Πανεπιστήμιο Κρήτης. Σχολή Θετικών και Τεχνολογικών Επιστημών. Τμήμα Φυσικής (2021).

[3] J. C. Allred, R. N. Lyman, T. W. Kornack, and M. V. Romalis, High-Sensitivity Atomic Magnetometer Unaffected by Spin-Exchange Relaxation, Physical Review Letters **89**, 130801 (2002).

[4] I. K. Kominis, T. W. Kornack, J. C. Allred, and M. V. Romalis, A subfemtotesla multichannel atomic magnetometer, Nature **422**, 596 (2003).

[5] S. Seltzer and M. Romalis, Unshielded three-axis vector operation of a spin-exchange-relaxation-free atomic magnetometer, Applied Physics Letters **85**, 4804 (2004).